Fibers and Polymers 2017, Vol.18, No.3, 424-433
DOI 10.1007/s12221-017-6983-4

ISSN 1229-9197 (print version)
ISSN 1875-0052 (electronic version)

Development and Evaluation of Novel Eucalyptus Essential Oil Liposomes/Chitosan Composite Sponges for Medical Use

Jiapeng Tang and Yan Ge[1]*

Department of Biochemistry and Pharmacy, Institute of Nautical Medicine, Nantong University, Nantong 226019, PR China
[1]School of Textile and Clothing, Nantong University, Nantong 226019, PR China
(Received October 7, 2016; Revised December 29, 2016; Accepted January 5, 2017)

Abstract: Novel eucalyptus essential oil liposomes (EEOLs)/chitosan composite sponges (EC) were successfully fabricated by electrostatic self-assembly. EEOLs were prepared by the thin-membrane hydration method with sonication and blended with chitosan solution to create the sponges by lyophilization. The observations of transmission electron microscopy (TEM) and scanning electron microscopy (SEM) confirmed the existence of eucalyptus essential oil in the lipid bilayer of liposomal membrane and the location of the liposomes in positive holes formed by the protonated amino groups of chitosan. The average size of EEOLs was about 60 nm. Fourier transform infrared (FTIR) analysis showed the destroy of inter- and intramolecular hydrogen bonding among chitosan chains and the construction of the intermolecular hydrogen bonding between chitosan and molecules on the surface of EEOLs. The incorporation of EEOLs in chitosan sponges slightly decreased the porosity, fluid absorptivity, gas permeability and hemostatic property of sponges, but increased their biodegradation ability. EC exhibited more rapid and efficient microbicidal effects against *Staphylococcus aureus* (*S. aureus*), *Pseudomonas aeruginosa* (*P. aeruginosa*) and *Candida albicans* (*C. albicans*) than pure chitosan sponges. EC showed no toxicity toward human HEK293T cells and no significant adverse effect on cell attachment and proliferation of HEK293T cells. This inherent behaviour can be exploited to apply in the medical field.

Keywords: Eucalyptus essential oil liposomes, Chitosan, Performance, Microbicidal activity, Biocompatibility

Introduction

Chitosan is a linear polysaccharide composed of randomly distributed β-(1-4)-linked D-glucosamine and N-acetyl-D-glucosamine. It is one of the most attractive hemostatic, antimicrobial, biocompatible and biodegradable polymers. Chitosan has been extensively applied in medical, food, chemical, cosmetics, water-treatment, metal extraction and recovery, biochemical and biomedical fields [1,2]. Lyophilization technique is one of the most promising methods to produce the porous bioactive materials. The chitosan sponges prepared by freeze-drying method have uniform pore size, interconnected channels, the controlled porosity, high specific surface area and good performances [3-5], which are conducive to cell adhesion growth and reproduction, the deposition of extracellular matrix, in and out of nutrients and oxygen, metabolites discharge, as well as the growth of blood vessels and nerve. Therefore, chitosan sponges as medical materials can protect the skin defect from infections, dehydration and subsequently tissue damage, which are more suitable for serious accidental injury or burning [6].

The antimicrobial activity of chitosan is dependent on content, molecular weight and deacetylated degree of chitosan, and medium pH [7-11], which greatly restrains the usage of chitosan. In general, the antimicrobial activity of chitosan materials is improved by three methods: grafting modification [12,13], encapsulating and structure alteration (nanofibrous membranes) [14,15]. Recently, the antimicrobial activity of the novel chitosan sponges has been enhanced by various antimicrobial agents, including sliver and natural antimicrobial agents [3-5]. The chitosan materials for essential oil delivery systems have also been discussed [16]. For example, oregano essential oil is encapsulted into chitosan nanoparticles by two-step method [17]. Eucalyptus essential oil (EEO), one of the natural antimicrobial agents is the volatile essential oil mainly derived from the leaves of Australian native plant *Eucalyptus globules* Labill. EEO has a history of wide application in pharmaceutical, antiseptic, repellent, flavouring, fragrance and industrial uses [18]. EEO possesses antimicrobial activity against bacteria, fungi and virus, consisting of soil-borne and post-harvest pathogens [19]. They can reduce mycelial growth of bacteria, interfere spore production and germination of fungi [20]. Furthermore, studies have also documented that EEO is effective against multidrug-resistant bacteria [21-23]. Additionally, the combinations of aromadendrene and 1,8-cineole, two constituents of EEO apparently exhibit synergistic and additive antimicrobial properties [22]. EEO has been successfully incorporated into the polymer for wound dressing application, such as occlusive or semiocclusive wound dressings [24] and disposable wound dressings [25]. However, EEO and its components are poisonous if taken in large quantities [26], especially for children [27]. The tissue fluid at the wound is a closed system so that the EEO released from the material will accumulate and directly contact with human cells, resulting in the unknown allergies and inflammatory reactions. Therefore, the release of EEO into the outside of material should be weakened as much as possible. It needs to design a

*Corresponding author: ntdxgeyan@126.com

material that can kill microorganisms in its interior and minimize the release of fungicides in material to avoid the side effects.

Liposome technology as a rapid-developped drug carrier technology has attracted wide attention due to its unique nature. Related researchers have made a lot of work in this field and produced novel essential oil liposomes in order to improve the stability, sustained release of essential oil and reduce its allergenicity [28]. In this study, spherical EEO liposomes (EEOLs) prepared by thin-film hydration method were firstly embedded into chitosan sponges. We attempted to improve the antimicrobial activity of chitosan wound dressings and alleviate the cytotoxicity of EEO.

Experimental

Materials

Chitosan (degree of deacetylation with acid-base titration method, 80.7±3.2 %, and molecular weight of 50 kDa), soya bean lecithin and cholesterol were supplied by Sinopharm Chemical Reagent Co., Ltd. (Shanghai, China). EEO was purchased from Nanning Innovative Pharmceutical Technology Co., Ltd. (Nanning, China). Concentrations of the EEO components determined by gas chromatographic analysis were as follows: 3.2 % α-pinene; 0.6 % β-pinene; 0.8 % β-myrcene; 0.5 % phellandrene; 90.0 % 1,8-cineole; 1.1 % γ-terpinene; 1.7 % α-terpineol. All other chemicals were analytical grade reagents. The water used for experiments was supplied by double distillation of deionized water.

EEOLs Preparation

The thin-membrane hydration method with bath-type sonicator [29] was used to prepare EEOLs. Briefly, 137.5 mg soya bean lecithin and 25 mg cholesterol were dissolved in chloroform (10 m*l*). The solvents were removed using a rotary evaporator (room temperature, 15 rpm, a high vacuum), resulting in a lipid thin film. The thin film was redissolved in 10 m*l* of 12.0 mmol/*l* phosphate-buffered saline (PBS, containing 0.8 % v/v Tween 80 and 1.2 % v/v EEO), pH 7.4, by agitation for 15 min at 55 °C. Simultaneously, the preparation sonication (300 W sonication power) was carried out in a bath-type sonicator (Branson Ultrasonics, Danbury, CT, USA) to form small unilamellar vesicles (SUVs). Finally, in order to anneal any structural defects, the liposomal dispersions prepared were stored at room temperature for 3 h.

EEOLs/chitosan Composite Sponges Fabrication

2.0 % w/v chitosan powder and 0.4 % v/v glycerol were dissolved in 1.0 % v/v acetic acid solution to obtain the transparent and homogeneous chitosan solution. Chitosan solution was mixed with EEOLs suspension in the volume ratio of 0.5:1, 1:1, 3:1 and 9:1 under vigorous stirring for 4 h, respectively. The resulting homogenous mixture was poured into a clean, sterile, glass Petri dish. The mixture was lyophilized at -80 °C to evaporate the utilized solvent from the system and obtain the flexible and porous EEOLs/chitosan composite sponges (EC0.5, EC1, EC3 and EC9). For comparison, EEOLs suspension was replaced by PBS and PBS containing 0.8 % v/v Tween 80, 1.2 % v/v EEO to prepare the pure chitosan sponges (PC1, PC3 and PC9) and chitosan sponges with EEO (PE1, PE3 and PE9) using the same lyophilization method above, respectively.

Characterization

The size and morphology of the EEOLs were studied using a transmission electron microscope (TEM; JEM-2100, Tokyo, Japan). The structural morphology of the sponges was observed by a scanning electron microscopy (SEM; JSM-6510, JEOL, Japan). Fourier transform infrared (FTIR) spectra were recorded on a Nicolet iS10 FTIR spectrometer (USA) in the range of 400-4000 cm^{-1}.

Zeta Potential of the Mixture of EEOLs and Chitosan

EEOLs suspension was mixed with chitosan solution in a certain ratio and then the mixture was diluted with water to the appropriate concentration. Zeta potential of the obtained mixture was measured by Zetasizer (Nano ZS90, Malvern, UK).

Measurements of Porosity

Porosity of the sponges was determined using liquid displacement method as described by Anisha *et al.* [30]. The sample was cut into 2 cm×2 cm and accurately weighed. Each piece was fully immersed with ethanol and weighed, then the wet piece was added into the pycnometer filling with ethanol and weighed. Porosity was calculated by the following formula (1):

$$\text{Porosity (\%)} = \frac{W_1 - W_0}{W_1 + W_2 - W_3} \times 100 \quad (1)$$

where W_0 is the weight of dry sponge, g; W_1 is the weight of wet sponge, g; W_2 is the weight of pycnometer filling with ethanol, g; W_3 is the weight of pycnometer filling with ethanol and wet sponge, g.

Performance Test of EC

The fluid absorption and water vapor transmission rate of samples were determined as described by Ge *et al.* [5]. The sponges were cut into 5 cm×5 cm pieces and each piece was immersed in a vial containing PBS (pH 7.4) solution and incubated at 37 °C for 30 min. PBS solution was used to simulate the tissue fluid at the wound. Then the swollen piece was withdrawn and wet weight of piece was measured after carefully removing its surface solution with a filter paper. Fluid absorption (FA) of sponges was defined by the average quality of absorbed solution for per gram of sponges and calculated using equation (2):

$$FA\ (\mathrm{g\cdot g^{-1}}) = \frac{W_w - W_d}{W_d} \quad (2)$$

where W_w is the weight of sample immersed in PBS at 37 °C for 30 min, g; W_d is dry weight of the sponge, g.

In addition, a circular piece of the specimen was fastened over the top of a cup (10 cm diameter) containing water. The sponge-cup was assembly weighed and then placed in an incubator of 20 % RH at 37 °C for 24 h, followed by weighing the sponge-cup assembly. The water vapor transmission rate (WVTR) was calculated using the following equation (3):

$$WVTR\ (\mathrm{g\cdot m^{-2}\cdot d^{-1}}) = \frac{W_4 - W_5}{ST} \quad (3)$$

where W_4 and W_5 are the weights of the film-cup assembly before and after incubation, respectively, g; S is the area of the rim of cup, m^2; T is the experimental time, d.

Hemostatic Effect Test

Hemostatic effect test was done based on the reported method by Anisha *et al.* [30]. The sponge was cut into a wafer of about 10.0 mm diameter and placed into 24 well plate, and prewarmed to 37 °C. Citrated whole blood (0.2 m*l*) was then dispensed onto the sponges and started coagulation by adding 5 μ*l* of 1.0 % w/v $CaCl_2$ solution. 1 m*l* PBS was added to hemolyze red blood cells (RBCs) that were not trapped in the clot. The solution from plate was diluted and centrifuged for 2 min at 500×*g*. The resulting hemoglobin concentration in the supernatant was indicated by the absorbance at 540 nm (UV-2450 spectrophotometry, SHIMADZU, Japan).

***In vitro* Lysozyme Biodegradation Test**

In vitro lysozyme biodegradation test of sponges was carried out as described by Huang *et al.* [31]. The sponge samples were equally weighed (0.2 g) and immersed in 30 m*l* of PBS with lysozyme (70,000 U/mg) and NaN_3 (0.5 mg/m*l*), then incubated at 37 °C. The sponges were removed, washed and freeze-dried after 7, 14, 21 and 28 d, respectively. The degradation of the sponges was calculated using the following formula (4):

$$\frac{\text{Remaining weight}}{\text{Original weight}}(\%) = \frac{W_l}{W_s} \times 100 \quad (4)$$

where W_l is the dry weight of the sponge after lyophilization, g; W_s is the dry weight of the initial sponge, g.

***In vitro* EEO Release from Sponges**

1,8-cineole, the main component of EEO was considered as the index of *in vitro* release of EEO from the sponges. 0.2 g sponges were suspended in 30 m*l* PBS (pH 7.4) and incubated at 37 °C, where 1,8-cineole was released into the buffer by diffusion. Like the determination of FA, PBS solution was used to simulate the tissue fluid at the wound. 10 μ*l* of buffer was removed to measure the concentration of released 1,8-cineole using gas chromatography every 12 h. The release of 1,8-cineole in the solution was observed over a period of 1 week.

1,8-cineole in the solution was determined by gas chromatography with n-dodecane as an internal standard. Gas chromatography appliances used included a Shimadzu GC-2014C system equipped with a fused-silica Stabilwax® column (60 m×0.32 mm i.d.; film thickness 0.50 μm) and a flame ionization detector (FID). Carrier gas was hydrogen at a constant voltage. The oven temperature programme was 75 °C for 4 min, then 4 °C/min until 200 °C was reached, and maintained 10 min. The detector and the injector temperatures were 250 °C. The volume of the injected sample was 0.2 m*l* and the split ratio was 1:50.

Microbicidal Activity of Sponges

The antimicrobial effects of EC were assessed according to the killing log values of the sponges against Gram-positive bacteria (*Staphylococcus aureus* ATCC 6538), Gram-negative bacteria (*Pseudomonas aeruginosa* ATCC 27853) and fungi (*Candida albicans* ATCC 10231). The sponge cut into a wafer of 1 cm diameter was put in the liquid culture, which was diluted to 5×10^7 cfu/m*l* with Luria Bertini broth (*S. aureus* and *P. aeruginosa*) and yeast extract-peptone-dextrose medium (*C. albicans*). The sample was cultured at 37 °C for 24 h and then living cell concentration was observed by a dilution plate counting method. Killing log value (KLV) of the sponges was calculated according to the following formula (5):

$$KLV = \log_{10}N_0 - \log_{10}N_t \quad (5)$$

where N_0 is the number of microorganism in broth at 0 contact time, cfu/m*l*; N_t is the number of microorganism in broth at the time, cfu/m*l*.

***In vitro* Effect of EEOLs on Cell Attachment and Proliferation**

The human embryonic kidney 293T (HEK293T) epithelial cells were used for studying *in vitro* effect of sponges on cell attachment and proliferation. The cells were maintained in Dulbecco's modified eagle medium (DMEM) with 10 % fetal bovine serum (FBS), 10 units/m*l* penicillin, 100 μg/m*l* streplomycin (HyClone Laboraturies, Inc., USA) at 37 °C in air (5 % CO_2). Cells were seeded onto 24 well plates with a seeding density of 4.0×10^4 cells/m*l* in a well. After the cell incubation of 24 h, the 1.0 cm-diameter sponges (PC1, PE1 and EC1) were added into the well and made sponges come into contact with the cells. The cells continuted to be cultured for 3 and 7 d, then the sponges were removed, respectively. The attachment and proliferation of cells were directly imaged using the microscope (DM4000B, Leica, German).

Results and Discussion

Morphology and Structure of EEOLs

EEOLs were prepared by thin film hydration and sonication technology. Figures 1(A)-(C) show the TEM images of blank liposomes (BLs). BLs suspension displayed that the hollow small single-chamber vesicles with smooth surface and the non-uniform particle size of 25-55 nm slightly aggregated. Figures 1(D)-(F) are TEM images of EEOLs suspension, showing the existence of two types of particles in EEOLs suspension. EEOLs were large spherical particles, approximately 60±5 nm of size, distributing uniformly without adhesion and agglomeration. The encapsulation efficiency of EEOLs prepared reached 97.35± 0.51 % (Table S1). The surface of EEOLs was concave-convex with uneven gray scale, even there were a lot of small particles with about 10 nm diameter in grain boundary. In addition, a number of dark spherical particles in about 10 nm size were distributed outside of EEOLs, which were EEO micelles coated with Tween 80. Firstly, EEO was coated in micelles formed by Tween 80, and then fused with blank liposome vesicles. Polyoxyethylene of Tween 80 extended and covered the liposome surface, resulting in the larger particle size. The surrounding of spherical liposome existed a ring shape, because liposome had the hollow vesicle structure and the ring was the bilayer of liposome. Two long alkyl chains in phospholipid molecules of lipid bilayer provided a hydrophobic platform, so EEO was embedded into continuous phospholipid bilayer with fusion. The uneven distribution of Tween 80 micelles in phospholipid bilayer caused non-uniform distribution of EEO in the liposome membrane, displaying the non-uniform gray scale

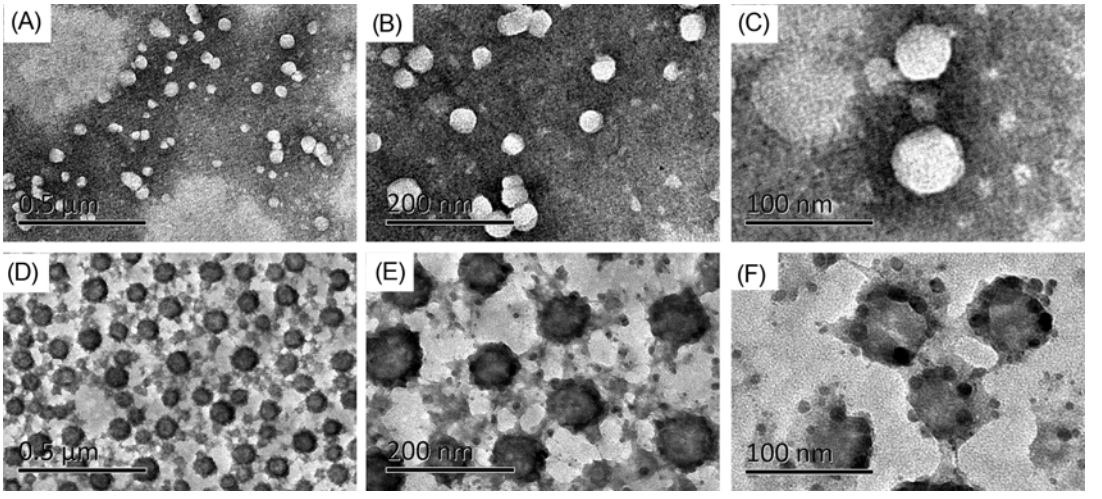

Figure 1. TEM photography of BLs (A-C) and EEOLs (D-F).

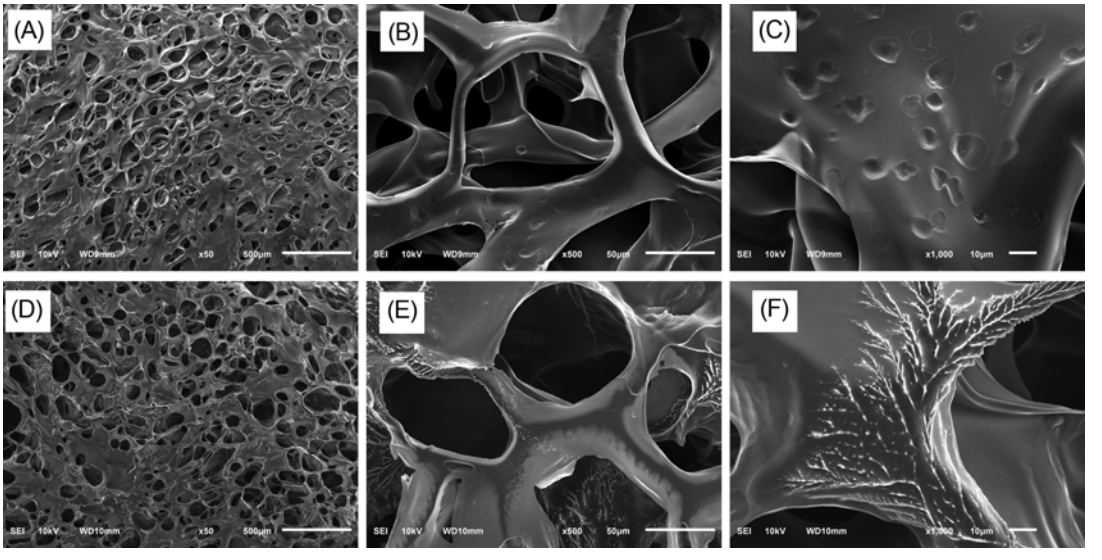

Figure 2. SEM photography of PC1 (A-C) and EC1 (D-F).

of EEOLs in Figure 1(F).

Morphology and Structure of PC and EC

Figure 2 shows the SEM images of PC1 and EC1. Both PC1 and EC1 had the three-dimensional fibrous network structure and their pore sizes were in the range of 50-80 μm. The frozen water engendered stress in the freezing process of chitosan solution, leading to the hollows on the surface of fibers. The surface morphology of EC1 was notably different from PC1. Hollows on the fiber surface gradually disappeared and were replaced by dendritic and radial bright stripes, which might relate to EEOLs distribution. Owing to the strong hydrogen bonding interactions among chitosan molecules and advanced film forming property of chitosan, chitosan spread and a thin chitosan layer was coated onto the pore edge, which was like chitosan/silk fibroin composite scaffolds [32].

FTIR Analysis

FTIR spectroscopy was used to examine the interactions between EEOLs and chitosan in Figure 3. Due to the intramolecular hydrogen bond of chitosan in the PC1, a broad characteristic peak at 3360 cm^{-1} was assigned to the associated N-H and O-H stretching vibration. The double peaks at 2860 cm^{-1} and 2920 cm^{-1} were attributed to C-H stretching vibration. The main absorption peaks of the sponge were observed at 1640 cm^{-1}, attributed to C=O stretching (amide I), at 1550 cm^{-1}, assigned to N-H bending (amide II), at 1410 cm^{-1}, assigned to C-N stretching and N-H bending (amide III). The intense peak located at 1070 cm^{-1} was ascribed to C-O-C stretching vibration on the ring. Another intense peak at 1020 cm^{-1} was assigned to C-O stretching and O-H bending of the primary alcohol. The peak at 896 cm^{-1} was assigned to β-glycosidic bond.

The absorption peaks of EC1 composite sponge displayed essentially in agreement with the PC1, but most of these peaks red-shifted. Compared the EC1 with PC1, the peaks of 3360 cm^{-1}, 2920 cm^{-1}, 2860 cm^{-1}, 1640 cm^{-1}, 1550 cm^{-1}, 1410 cm^{-1} and 1070 cm^{-1} shifted to 3250 cm^{-1}, 2910 cm^{-1}, 2840 cm^{-1}, 1630 cm^{-1}, 1540 cm^{-1}, 1400 cm^{-1} and 1060 cm^{-1}, respectively. EEOLs were incorporated into chitosan molecules to destroy the intramolecular hydrogen bond of chitosan and rebuild the intermolecular hydrogen bonds between chitosan and molecules on the surface of EEOLs. The formation of hydrogen bonds increased the length of O-H, N-H, C-N, and C=O bonds, reducing the bond force constant and causing the stretch vibrational frequency of the peaks to move towards the lower wavenumber [33].

Zeta Potential of the Mixture of EEOLs and Chitosan

Zeta potential of the mixture solution of EEOLs and chitosan in different ratios was measured to explain their interaction and the results are presented in Figure 4. Zeta potential of EEOLs suspension is -7.97 mV and that of chitosan solution is +25.29 mV. The data showed that the surface of EEOLs had lots of negative charges in the suspension and chitosan in solution carried a high positive charge density. When the environment pH was less than the pKa of chitosan, the amino group in the D-glucosamine units, a monomer of chitosan, was protonated and carried a positive charge. The coating mechanism or interaction of chitosan and liposomes mainly depends on electrostatic forces [34]. When the chitosan solution mixed with liposomal suspension, chitosan molecule whose charge polarity was opposite to the charges of liposome surface, namely positive counterions, readily bounded to negatively charged surfaces of liposomes [35]. The positive charge density near the surface of EEOLs exceeded that in the bulk phase due to the agglomeration effect. The counterions were aggregated on EEOLs surface to screen the negative charges and Zeta potential of the system decreased until it reached zero. However, the increase ratio of chitosan subsequently led to protonation of the amino groups in the supersaturated

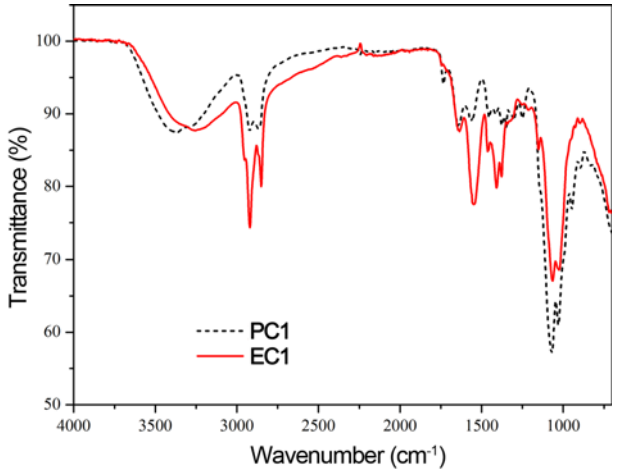

Figure 3. FTIR spectra of PC1 sponge and EC1 composite sponge.

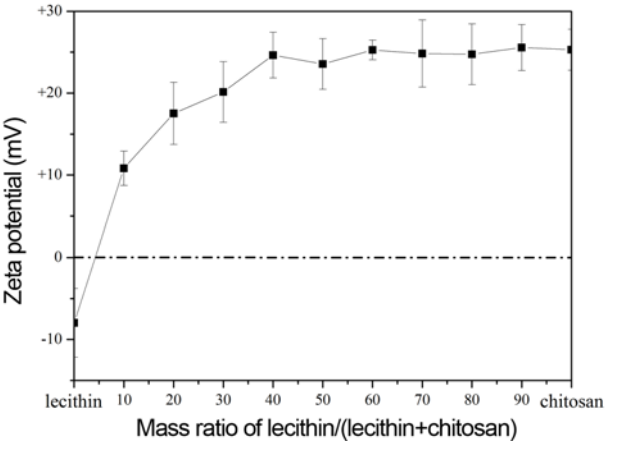

Figure 4. Zeta potential of the mixture of EEOLs and chitosan.

chitosan, causing a positive Zeta potential of the mixed solution. The positive Zeta potential rose steadily with the further increase in chitosan to reach that of pure chitosan solution eventually. Therefore, it was speculated that EEOLs combined with chitosan in the solution through electrostatic self-assembly and were firmly located at "positive holes" weaved by the chitosan chain using the freeze-drying method.

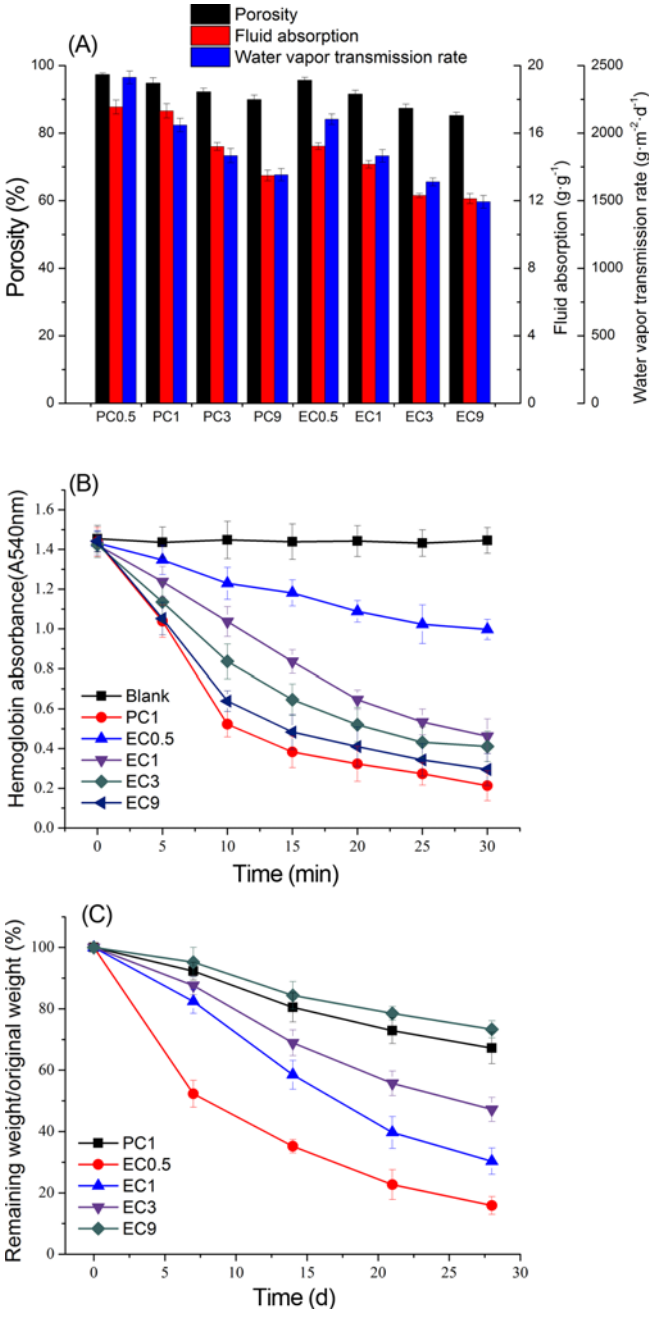

Figure 5. (A) The porosity, fluid absorption and water vapor transmission rate of chitosan-based sponges, (B) blood clotting rates of wound dressings, as measured by absorbance of hemoglobin from lyzed uncoagulated red blood cells, and (C) remaining weights of chitosan-based sponges for each time interval incubated in PBS with 0.5 mg/m*l* lysozyme at 37 °C.

Porosity, FA and WVTR of PC and EC

According to the data presented in Figure 5(A), chitosan-based sponges have very high porosity. The porosity of EC and PC increased with the decrease in the proportion of chitosan solution. When chitosan solution was mixed with PBS in an equal volume, the porosity of PC1 prepared was 94.8±1.6 %. When PBS was replaced by EEOLs suspension, the porosity of sponge dropped slightly to 91.5±1.2 %, remaining over 90 %. The proportion of chitosan solution continued to increase so that the porosity of EC tailed off to below 90 %. FA and WVTR of chitosan-based sponge mainly depend on the porosity, so FA and WVTR of PC and EC sponges gradually increased with the increase of porosity. Due to the amino group and hydroxyl group of chitosan, chitosan-based sponge had good hydrophilicity. When chitosan solution was mixed with an equal volume of PBS, FA of PC1 prepared was 17.32±0.42 $g \cdot g^{-1}$. When EEOLs suspension replaced PBS, liposomes were incorporated into chitosan sponges, which prohibited chitosan-based sponges from moistening and swelling, decreasing the fluid absorption due to the hydrophobic property of liposomes [36]. Thus, FA of EC1 declined to 14.16±0.22 $g \cdot g^{-1}$, lower than PC1 (17.32±0.42 $g \cdot g^{-1}$). Owing to hydrophilicity of EEOLs, WVTR of EC1 was around 1832 $g \cdot m^{-2} \cdot d^{-1}$, also lower than PC1 (about 2060 $g \cdot m^{-2} \cdot d^{-1}$), but WVTR of EC1 still remained an appropriate level [37].

Hemostatic Effect and *in vitro* Biodegradation of Sponges

The absorbance of hemoglobin solution at 540 nm was positively correlated with the hemoglobin concentration. When blood was handled with the material, low absorption value of blood indicated low hemoglobin concentration and reflected excellent hemostatic property of material under the same conditions. We used this method to study the effect of EEOLs incorporation on hemostatic performance of chitosan-based sponge. Chitosan has good hemostatic property as the ideal substrate of wound dressing [31,38]. Therefore, Figure 5(B) shows that PC1 owns excellent hemostatic property. The amino group in chitosan protonated in acidic and neutral solution, and interacted with the receptor of neuraminic acid residues with negatively charge on cell surface to make erythrocytes crosslink with chitosan and prompt the cells adhesion or the formation of three-dimensional network structure in the cross-linking reaction, capturing erythrocytes to be gathered [39]. However, when PBS solution was replaced by EEOLs suspension, the hemostatic performance of chitosan-based sponge EC1 declined. Soybean lecithin contained the impurities such as phosphatidic acid and phosphatidylinositol to cause the negative charges of EEOLs surface, which was proved by Zeta potential of EEOLs [40].

These negative charges could improve the stability of EEOLs and prevent the fusion of liposomes. But the electrostatic attraction between the negative charges and the protonated amino groups of chitosan blockaded the partial amino groups of chitosan, causing the reduction in blood coagulation rate of EC. Moreover, hemostatic performance of EC sponges declined with the increased ratio of EEOLs. The blood coagulation rate of material is critical to wound dressing. In order to compensate for the defects of EC in the coagulation rate, we will tend to use the high deacetylated degree of chitosan or modify the freeze-dry processing technology to improve positive charges on the surface of EC and strengthen its blood coagulation. In addition, it is also an alternative method to add the combined hemostatic agents to the material, including antifibrinolytics, blood coagulation factors, fibrinogen, and vitamin K.

Chitosan molecules can be effectively degraded to the soluble oligosaccharides with low molecular weight by lysozyme which catalyzes hydrolysis of β-1,4-linkages between D-glucosamine and N-acetyl-D-glucosamine residues in chitosan [41]. The difficulty degree in the diffusion of enzyme into material interior and the arrival of enzyme to reaction site determined the degradation rate of chitosan-based sponges in the process of heterogeneous enzyme reaction [42,43]. Figure 5(C) shows that EC1 loses a total weight of 69.7 % after the treatment of lysozyme for 28 d, which demonstrates the good degradability. But PC1 containing the same content of chitosan solution as EC1 loses a total weight of 32.8 %. Moreover, the degradation rate of chitosan-based sponges is accelerated with the increasing of EEOLs concentration. It was because that EEOLs addition weakened hydrogen bonding among chitosan molecules and destroyed regular arrangement of chitosan molecules, causing the partial disintegration of crystalline regions. The entire structure of material became loose so that to make lysozyme more rapidly diffuse into the reaction site and accelerate the reaction rate. Furthermore, the entanglement of chitosan molecules had adverse effect on lysozyme penetration. Seen from Figure 5(C), the degradation rate of EC9 is even slower than PC1. The enzymatic reaction rate of polymer degradation and the collapse of material structure were also highly interrelated and mutually reinforced. The intermolecular interaction among chitosan molecules was cracked and chitosan chains were also disentangled in addition of EEOLs, contributing to lysozyme penetration. So EC would own the better biodegradable property.

EEO Release of EC and PE

Figure 6 shows the release of 1,8-cineole from EC and PE. 1,8-cineole in the PE quickly diffused to material outside, and finally completely spread to establish the equilibrium of 1.8-cineole concentration between the internal and external of the material. The initial diffusion rate of 1,8-cineole in PE decreased with the increasing content of chitosan solution. It

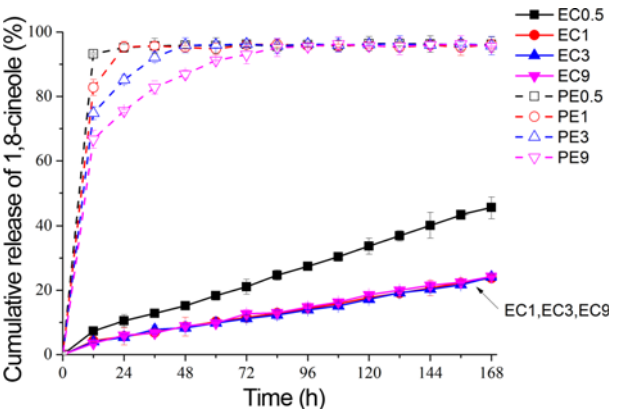

Figure 6. Cumulative release of 1,8-cineole over time from EC sponges and PE sponges.

was because that high chitosan concentration led to the more compact structure of sponge, weakening the EEO diffusion. However, 1,8-cineole in EC continuously released at nearly constant and slow rate and penetrated into the outside of material. This contributed to the encapsulation effect of liposome and stabilization effect of chitosan on liposome. Moreover, when the volume concentration of chitosan solution reached more than 50 %, the EEO release rate remained only about 3 %·d^{-1}. The sustained release of EEO could weaken the influence of EEO on the cells outside the sponge. The large EEOLs proportion also accelerated the release of EEO due to loose structure of sponges.

Microbicidal Properties of EC

According to papers published previously, the chitosan film containing thyme oil exhibited the growth inhibition effects against the gram negative microorganisms of *Escherichia coli* (*E. coli*), *Klebsiella pneumoniae*, *P. aeruginosa* and the gram positive microorganism of *S. aureus* [44]. The minimum inhibitory concentration of tea tree essential oil against *S. aureus* in chitosan/poly-caprolactone nonwoven mats was 24 % lower than the essential oil itself due to the chemical synergies [45]. The chitosan film containing tea tree oil showed sustained growth inhibitory effect against *S. aureus*, *E. coli* and *C. albicans* [5]. In this study, microbicidal capabilities of PC, EC and PE with the same chitosan concentration were compared based on the reported method by Doulabi *et al.* [46]. The three microorganisms, *S. aureus*, *P. aeruginosa* and *C. albicans* are the most common pathogens in human pyogenic infection, which can cause local pyogenic infection. *S. aureus*, a Gram-positive bacteria and *P. aeruginosa*, a Gram-negative bacteria are prokaryotic microorganisms and *C. albicans* is a kind of eukaryotic microorganism. KLVs of PC1 against *S. aureus*, *P. aeruginosa* and *C. albicans* were over 3 after treating for 16 h in Figure 7, which indicated that chitosan had a role in killing three microorganisms. PBS

solution was replaced by EEOLs suspension so that to improve the microbicidal efficiency of chitosan sponges. The results indicated that EEO played an important role in the microbicidal capability of the sponges. KLV of EC1 against *S. aureus*, *P. aeruginosa* and *C. albicans* reached or exceeded 5 after treatment for 12 h, which exhibited rapid and efficient killing efficiency. The microbicidal capability of EC1 was similar to that of PE1 except for *P. aeruginosa*. The bactericidal effect of EC1 against *P. aeruginosa* was better than that of PE1. It was probably that liposomes promoted the permeability of EEO to cell membrane.

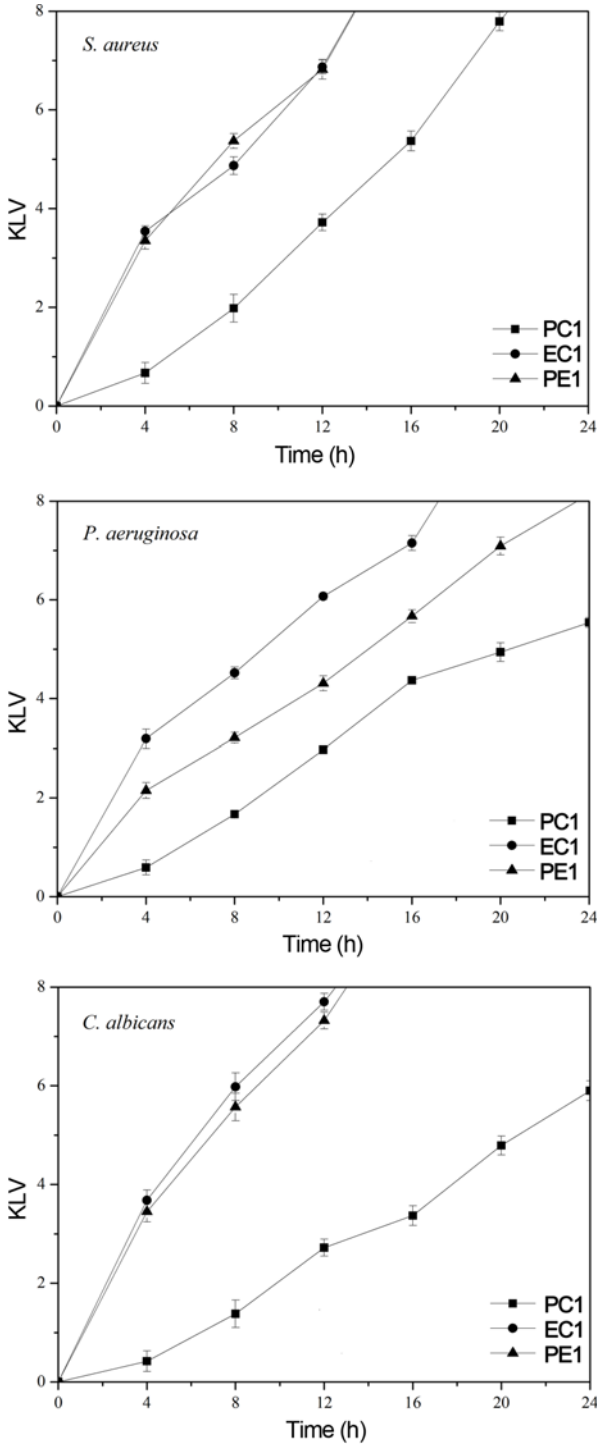

Figure 7. Microbicidal property of the sponges. Killing log values were measured after the treatment with sponges.

Effect of EEO Incorporation Style in Chitosan Sponge on Cell Attachment and Proliferation

The effect of essential oil incorporation style in material on cell adhesion and proliferation was analyzed according to cell morphology and growth using PC1 treatment as the control. The morphological and spreading patterns of the cells were observed after 0, 3 and 7 d of treatment (Figure 8). There was no significant difference in morphology and number of cells before treated by the three sponges (0 d). After 3 and 7 d, the cells treated with EC1 were well attached and showed excellent spreading, which were triangular or polygonal. The morphology and number of cells were similar to the control group (PC1). It indicated that EEOLs had no obvious inhibitory effect on cell morphology, adhesion and proliferation in short (3 d) and long term (7 d), and EC1 had good biocompatibility. But most of the cells treated with PE1 were dead. This could be due to the electrostatic self-assembly by which chitosan molecules enwrapped EEOLs in EC1 to alleviate the release of EEO into solution and the allergenicity effect of EEO on the HEK293T cells. According to Table S1, the encapsulation efficiencys and loading percents of 1,8-cineole in EC were similar with PE and only slightly higher than the PE. The incorporation of EEOLs into chitosan sponges could play an important role in attenuating the allergenicity of EEO to epithelial cells. Chitosan molecules were cross-linked and not easily eroded. EEOLs encapsulated with EEO were likely to be firmly embedded and immobilized in cationic holes cross-linked chitosan molecules by electrostatic self-assembly. However, EEO in the PE1 was loosely distributed in the chitosan molecules, exhibiting poor adhesion. EEO released into the media due to the concentration gradient of oil and the released 1,8-cineole concentration from PE1 was higher in the media than that from EC1 (Figure 9). EEO rapidly diffused into the medium and produced cytotoxic effects on cells. Therefore, the toxicity of free EEO to cells was significantly higher than EEOLs in chitosan-based sponges. The incorporation of EEOLs on the chitosan-based sponge could be the key factor to weaken the adverse effect of EEO on cell attachment and maintain the proliferation.

Conclusion

In this study, EC were prepared by electrostatic self-assembly and lyophilization consolidation. In comparison to porous PC, the decreased porosity of EC led to a slight decline trend in fluid absorption, water vapor permeability

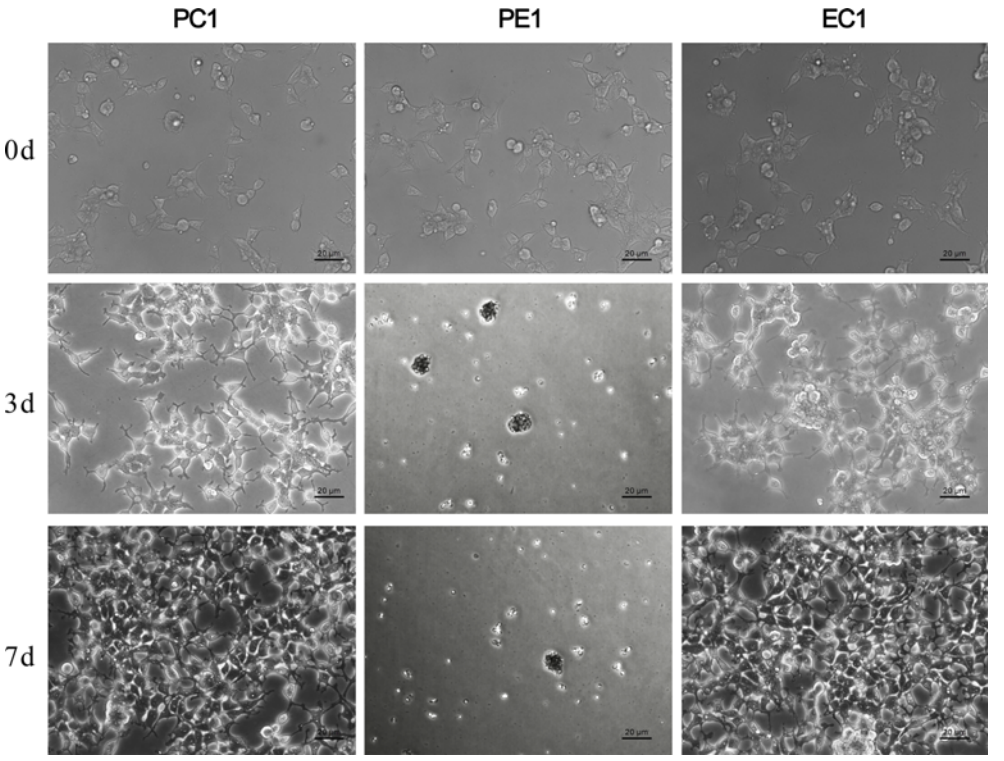

Figure 8. Microscopic images of HEK293T cells attachment and proliferation after the treatment of 0 d, 3 d, and 7 d with PE1 and EC1 sponges. The cells treated with PC1 served as the control. Scale bar denotes 20 μm.

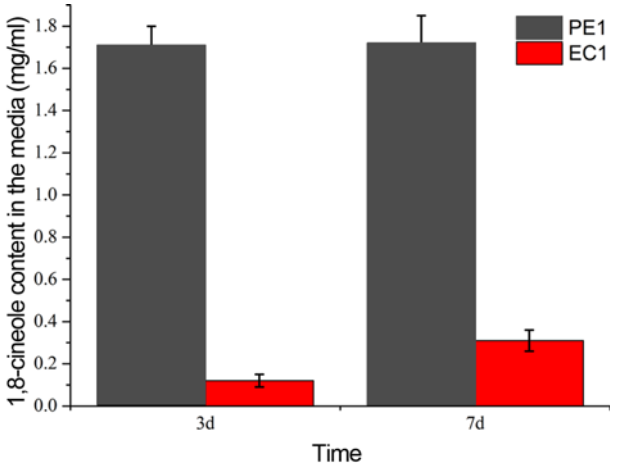

Figure 9. The concentration of 1,8-cineole released from the sponges to the media.

and hemostatic property. However, the degradability of EC was improved. Furthermore, the microbicidal efficiency of PC against *S. aureus*, *P. aeruginosa* and *C. albicans* was significantly enhanced with the incorporation of EEOLs and resembled PE. The attachment and growth of cells treated with EC was normal and preceded PE. From the results above, we can refer to the conclusion that EC would be a potential candidate for medical use.

Acknowledgements

This work was supported by Applied Research Program of Nantong City (MS12015065), Open Project Program of Large Instruments and Equipments of Nantong University (KFJN1625) and Natural Science Research Program of Nantong University (13ZJ006).

Electronic Supplementary Material (ESM) The online version of this article (doi: 10.1007/s12221-017-6983-4) contains supplementary material, which is available to authorized users.

References

1. M. Kong, X. G. Chen, K. Xing, and H. J. Park, *Int. J. Food Microbiol.*, **144**, 51 (2010).
2. D. Raafat, K. Von Bargen, A. Haas, and H.-G. Sahl, *Appl. Environ. Microbiol.*, **74**, 3764 (2008).
3. D. H. Li, J. L. Diao, J. T. Zhang, and J. C. Liu, *J. Nanosci. Nanotechnol.*, **11**, 4733 (2011).
4. T. Phaechamud and J. Charoenteeraboon, *AAPS PharmSciTech*, **9**, 829 (2008).
5. Y. Ge and M. Ge, *Fiber. Polym.*, **16**, 308 (2015).
6. C. Chen, L. Liu, T. Huang, Q. Wang, and Y. Fang, *Int. J. Biol. Macromol.*, **62**, 188 (2013).
7. Y. Omura, M. Shigemoto, T. Akiyama, H. Saimoto, Y.

Shigemasa, I. Nakamura, and T. Tsuchido, *Biocontrol Sci.*, **8**, 25 (2003).
8. L. J. R. Foster and J. Butt, *Biotechnol. Lett.*, **33**, 417 (2011).
9. L. Y. Zheng and J. F. Zhu, *Carbohydr. Polym.*, **54**, 527 (2003).
10. C. Qin, H. Li, Q. Xiao, Y. Liu, J. Zhu, and Y. Du, *Carbohydr. Polym.*, **63**, 367 (2006).
11. Y. J. Jeon, P. J. Park, and S. K. Kim, *Carbohydr. Polym.*, **44**, 71 (2001).
12. J. Li, D. Liu, C. Hu, F. Sun, W. Gustave, H. Tian, and S. Yang, *Carbohydr. Polym.*, **136**, 1137 (2016).
13. D. Zhang, W. Zhou, B. Wei, X. Wang, R. Tang, J. Nie, and J. Wang, *Carbohydr. Polym.*, **125**, 189 (2015).
14. W. A. Sarhan and H. M. Azzazy, *Carbohydr. Polym.*, **122**, 135 (2015).
15. B. P. Antunes, A. F. Moreira, V. M. Gaspar, and I. J. Correia, *Carbohydr. Polym.*, **130**, 104 (2015).
16. A. S. Pedro, E. Cabral-Albuquerque, D. Ferreira, and B. Sarmento, *Carbohydr. Polym.*, **76**, 501 (2009).
17. S. F. Hosseini, M. Zandi, M. Rezaei, and F. Farahmandghavi, *Carbohydr. Polym.*, **95**, 50 (2013).
18. T. D. Dhumal and J. Waghmare, *Int. J. Pharm. Sci. Res.*, **6**, 857 (2015).
19. D. R. Batish, H. P. Singh, R. K. Kohli, and S. Kaur, *Forest. Ecol. Manag.*, **256**, 2166 (2008).
20. A. C. G. Fiori, K. R. F. Schwan-Estrada, J. R. Stangarlin, J. B. Vida, C. A. Scapim, M. E. S. Cruz, and S. F. Pascholati, *J. Phytopathol.*, **148**, 483 (2000).
21. E. Sherry, H. Boeck, and P. H. Warnke, *Am. J. Infect. Control*, **29**, 346 (2001).
22. S. Mulyaningsih, F. Sporer, S. Zimmermann, J. Reichling, and M. Wink, *Phytomedicine*, **17**, 1061 (2010).
23. N. Trivedi and S. Hotchandani, *Indian J. Pharmacol.*, **36**, 93 (2004).
24. R. Khajavi, M. Abbasipour, M. G. Barzi, A. Rashidi, M. K. Rahimi, and H. H. Mirzababa, *Adv. Polym. Tech.*, **33**, 68 (2014).
25. I. Liakos, L. Rizzello, D. J. Scurr, P. P. Pompa, I. S. Bayer, and A. Athanassiou, *Int. J. Pharm.*, **463**, 137 (2014).
26. C. Regnault-roger, *Integr. Pest Manage. Rev.*, **2**, 25 (1997).
27. W. E. Foggie, *Brit. Med. J.*, **1**, 359 (1911).
28. M. Sherry, C. Charcosset, H. Fessi, and H. Greige-Gerges, *J. Liposome Res.*, **23**, 268 (2013).
29. Y. Ge and M. Ge, *J. Liposome Res.*, **25**, 222 (2015).
30. B. S. Anisha, R. Biswas, K. P. Chennazhi, and R. Jayakumar, *Int. J. Biol. Macromol.*, **62**, 310 (2013).
31. X. F. Huang, Y. F. Sun, J. Y. Nie, W. T. Lu, L. Yang, Z. L. Zhang, H. P. Yin, Z. K. Wang, and Q. L. Hu, *Int. J. Biol. Macromol.*, **75**, 322 (2015).
32. S. Y. Guang, Y. An, F. Y. Ke, D. M. Zhao, Y. H. Shen, and H. Y. Xu, *J. Appl. Polym. Sci.*, **132**, 42503 (2015).
33. X. Li, M. S. Yang, X. Shi, X. X. Chu, L. Chen, Q. Wu, and Y. Y. Wang, *Physica E-Low-Dimensional Systems & Nanostructures*, **69**, 237 (2015).
34. J. Thongborisute, H. Takeuchi, H. Yamamoto, and Y. Kawashima, *Pharmazie*, **61**, 106 (2006).
35. S. Jeon, C. Y. Yoo, and S. N. Park, *Colloid Surf. B-Biointerfaces*, **129**, 7 (2015).
36. M. Rennukka and A. A. Amirul, *Polym. Bull.*, **70**, 1937 (2013).
37. F. L. Mi, S. S. Shyu, Y. B. Wu, S. T. Lee, J. Y. Shyong, and R. N. Huang, *Biomaterials*, **22**, 165 (2001).
38. T. H. Dai, M. Tanaka, Y. Y. Huang, and M. R. Hamblin, *Expert Rev. Anti Infect. Ther.*, **9**, 857 (2011).
39. P. R. Klokkevold, P. Subar, H. Fukayama, and C. N. Bertolami, *J. Oral Maxillofac. Surg.*, **50**, 41 (1992).
40. T. Imura, K. Otake, S. Hashimoto, T. Gotoh, M. Yuasa, S. Yokoyama, H. Sakai, J. F. Rathman, and M. Abe, *Colloid Surf. B-Biointerfaces*, **27**, 133 (2003).
41. S. M. Lim, D. K. Song, K. J. Cho, S. H. Oh, D. S. Lee-Yoon, E. H. Bae, and J. H. Lee, *3rd Kuala Lumpur International Conference on Biomedical Engineering*, **15**, 94 (2007).
42. G. F. Picheth, M. R. Sierakowski, M. A. Woehl, L. Ono, A. R. Cofre, L. P. Vanin, R. Pontarolo, and R. A. De Freitas, *J. Pharm. Sci.*, **103**, 3958 (2014).
43. T. Honma, L. Zhao, N. Asakawa, and Y. Inoue, *Macromol. Biosci.*, **6**, 241 (2006).
44. D. Altiok, E. Altiok, and F. Tihminlioglu, *J. Mater. Sci. Mater. Med.*, **21**, 2227 (2010).
45. M. Y. Bai, T. C. Chou, J. C. Tsai, and H. C. Yang, *Mat. Sci. Eng. C-Mater.*, **33**, 224 (2013).
46. A. H. Doulabi, H. Mirzadeh, M. Imani, and N. Samadi, *Carbohydr. Polym.*, **92**, 48 (2013).